

Theoretical Study of Intermolecular Interactions in Benzopyrans Substituted with Polyhaloalkyl Groups [†]

Lisette A. Haro-Saltos, Pablo M. Bonilla-Valladares and Christian D. Alcívar-León *

Facultad de Ciencias Químicas, Universidad Central del Ecuador, Francisco Viteri s/n y Gilberto Gato Sobral, Quito 170521, Ecuador; laharo@uce.edu.ec (L.A.H.-S.); pmbonilla@uce.edu.ec (P.M.B.-V.)

* Correspondence: cdalcivar@uce.edu.ec

[†] Presented at the 28th International Electronic Conference on Synthetic Organic Chemistry (ECSOC 2024), 15–30 November 2024; Available online: <https://sciforum.net/event/ecsoc-28>.

Abstract: A study of the solid-state intermolecular interactions of twenty-nine benzopyrans substituted with polyhaloalkyl groups was carried out by quantum chemical calculations using the Mercury and WinGX computer programs. Molecular structures were obtained from crystallographic information files (CIF) of the CCDC database. C-H—O, C-H—X, C-X—O and C-X—X type contacts, characterized as unconventional hydrogen bonds, were identified and calculated. The criteria used for distances and angles were $d(D-A) < R(D) + R(A) + 0.50$ and $d(H-A) < R(H) + R(A) - 0.12^\circ$, where $D-H-A > 100.0^\circ$. D is the donor atom, A is the acceptor atom, R is the Van der Waals radius and d is the interatomic distance. In addition, Etter's notation was used to describe sets of hydrogen bonds in organic crystals, detailing the intermolecular contacts and periodic arrangements of the crystal packing. It was corroborated that certain positions of halogen atoms and their interactions play an important role in stabilizing the crystal lattice.

Keywords: crystal structure; intermolecular interaction; hydrogen bonding; computational chemistry; halogen bonds; chromones

Citation: Haro-Saltos, L.A.; Bonilla-Valladares, P.M.; Alcívar-León, C.D. Theoretical Study of Intermolecular Interactions in Benzopyrans Substituted with Polyhaloalkyl Groups. *Chem. Proc.* **2024**, *6*, x. <https://doi.org/10.3390/xxxxx>

Academic Editor(s): Name

Published: 15 November 2024



Copyright: © 2024 by the authors. Submitted for possible open access publication under the terms and conditions of the Creative Commons Attribution (CC BY) license (<https://creativecommons.org/licenses/by/4.0/>).

1. Introduction

The molecular study of chromones and their derivatives has garnered significant interest in recent years [1,2], particularly structures that incorporate perhaloalkyl groups as -CF₃, -CF₂Cl, -CF₂CF₃, -CCl₂H [3–5] and halogen atoms (-F, -Br, -Cl, -I) in the benzopyrone ring [6]. In this sense, the introduction of halogen atoms has been shown to enhance biological properties as lipophilicity [7] that played a great role in the fields of anticancer, antibacterial, and antiviral drug discovery [8]. Moreover, the halogen atoms generate interesting crystalline packing as halogen bonding interactions, classified as weak to medium-strength non-covalent forces that work synergistically with hydrogen bonds, imparting molecules with notable pharmacokinetic properties and making them attractive for the development of new materials [9]. In addition to halogen bonds, non-classical hydrogen bonds and other interactions, such as $\pi-\pi$ stacking and C-H— π interactions, play a crucial role in describing and controlling the crystal structure [9,10].

This study focuses on 29 polyhaloalkyl-substituted benzopyran compounds, with crystallographic data obtained from the Cambridge Crystallographic Data Center (CCDC). Molecular stacking analysis and Hirshfeld surface calculations were performed using Mercury, PLATON, and Crystal Explorer software, with compound 8 selected as a representative example for discussing the geometric and energetic parameters.

2. Materials and Methods

A random search of articles was performed using keywords such as “haloalkylchromones” and “chromones” to obtain a crystallographic codes of crystal structures featuring the heterocycle benzopyran chromone, which is composed of an aromatic ring fused to a 4-pyran ring. Subsequently, CIF files were downloaded from the Cambridge Crystallographic Data Center (CCDC). A total of 29 molecules were processed with the programs Mercury 2022.3.0, PLATON for Windows (v1.17.53 of WinGX) and Crystal Explorer 3.1, in order to elaborate molecular plots, calculate geometrical parameters and generate Hirshfeld surfaces, respectively. For hydrogen bonds, the following criteria were used: $d(D-A) < R(D) + R(A) + 0.50 \text{ \AA}$ and $d(H-A) < R(H) + R(A) - 0.12 \text{ \AA}$, with an angle $D-H-A > 100.0^\circ$. D is the donor atom, A the acceptor, R the van der Waals radius and d the interatomic distance. In the representation of short contacts, those smaller than the sum of the Van der Waals radii + 0.3 Å were considered. Etter’s notation $R_d^a(r)$ was used to describe hydrogen bond sets in organic crystals, where R represents the ring, r the number of atoms in the ring, a the acceptor atoms and d the donors. Hirshfeld surfaces include the descriptors d_{norm} (normalized contact distance), *curvedness index* and *shape index*, which provide information about the chemical behavior of the molecule. The d_{norm} surface highlights intermolecular interactions: red areas indicate short contacts, white areas common contacts, and blue areas long contacts. The 2D fingerprint plots depict d_e/d_i interactions in the range of 0.8 to 2.6 Å, including reciprocal contacts. The 3D d_{norm} surfaces are mapped over a fixed color scale of -0.243 au (red) -0.824 au (blue) Å, *shape index* in the color range of -1.0 au (concave) -1.0 au (convex) Å, and *curvedness index* in the range of 14–4.0 au (flat) -0.4 au (singular) Å. The surface properties above mentioned (d_{norm} , *shape* and *curvedness index*) were used to identify planar stacking. Intermolecular interaction energies were calculated using monomeric wave functions at the HF/3-21G level, obtaining accurate values of electrostatic, polarization, and repulsion energies for molecules separated by no more than 3.8 Å within the cluster.

3. Results and Discussion

3.1. Crystalline Structure, Supramolecular Features and Intermolecular Interactions

Chromones are a group of heterocyclic compounds, generally named as chromen-4-one. Various syntheses have incorporated halogen atoms into the phenyl ring of the chromone, which generates interesting interactions. Using the hydrogen and halogen bonding interactions (A° , $^\circ$) and their energies (kJ/mol) a 3D scatter plot (Figure 1) was generated to visualize the relationship between the distances R (X axis), the total energy ETOT (Y axis), and the index of each point (Z axis, used as a placeholder in the absence of angle data). The color of the dots indicates the ETOT values, with warm colors representing higher energies and cool colors for lower energies. The generated 3D scatter plot allows to discuss the relationship between the geometrical parameters (bond distances and angles) and the interaction energies (especially the total energy, ETOT) in the hydrogen-halogen interactions observed in the compounds 1–29. As seen in the graph, as the distance R increases, the total energy ETOT tends to increase towards less negative values (closer to zero), indicating a decrease in the stability of intermolecular interactions. In this sense, stronger and more stabilizing interactions tend to occur at shorter distances, while weaker interactions, such as halogen-halogen interactions, occur at longer distances. Shorter interactions, with R values around 2.4–2.6 Å, show more negative ETOT energies (values between -17 and -30 kJ/mol), indicating that these interactions are significantly stabilizing. This suggests that the studied hydrogen and halogen bonds are well positioned geometrically in the crystal packing to optimize the stabilization of the supramolecular network in the crystal structures of the studied chromone heterocycles. Furthermore, as R exceeds 3 Å, ETOT values approach zero or even exhibit positive values, indicating that interactions at these distances are much weaker and less stabilizing. This can be attributed to halogen-halogen interactions, which are generally less energetically

favorable compared to hydrogen bonds. Some extremely negative values (such as those found in compound 25, with ETOT = -129,216.2 kJ/mol) reflect outliers in the energy calculations that are not representative of typical intermolecular bond energies. Likewise, with respect to Variability in Total Energy Values (ETOT) the energies vary from approximately -30 kJ/mol to values close to 0 kJ/mol, suggesting a diversity of interaction types. Interactions with more negative values (e.g., -17.5 kJ/mol in Compound 1) tend to correlate with shorter distances, reinforcing the idea that shorter bonds are more energetically favorable. Regarding the effect of distances and angles on energy, it is observed that angles closer to 180° (as in the case of some hydrogen bonds with angles of 169°) tend to be associated with stronger interactions and more negative ETOT values. This type of linear geometry optimizes orbital overlap and strengthens the intermolecular interaction. In contrast, interactions with smaller angles tend to be weaker, as suggested by the case of some halogen-halogen interactions in the analyzed compounds.

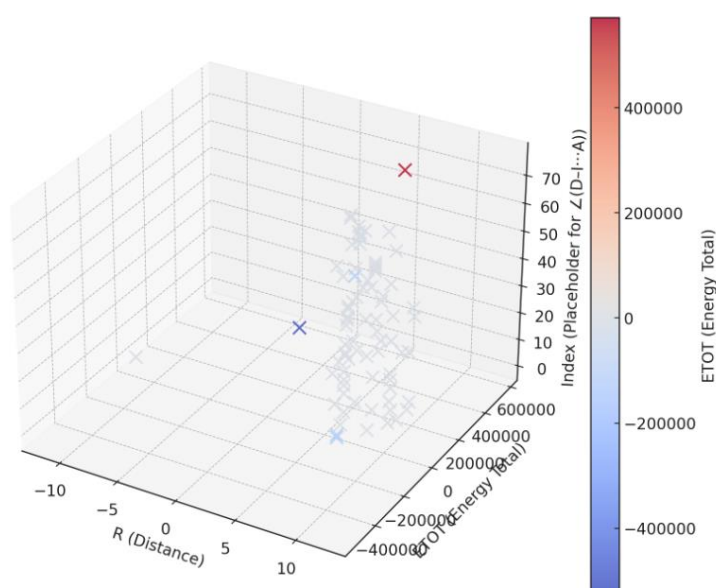


Figure 1. 3D Scatter Plot: R vs ETOTAL with color coding for 1–29 compounds.

On the other hand, energy data broken down into electrostatic (E_{elec}), polarization (E_{pol}), dispersive (E_{dis}) and repulsive (E_{rep}) energies indicate that dispersive and electrostatic energies are the main contributors to stabilization. Repulsive interactions, although present, tend to be less significant at optimal binding distances, while polarization energies tend to be lower. Dispersive contributions, especially, play a crucial role in halogen-halogen interactions, while hydrogen interactions show higher contributions from electrostatic energy due to the higher polarity of these bonds.

Figure 2 shows geometric parameters of π - π interactions kind stacking of the 1, 3–16, 20–23, 25 and 26 compounds. The distances between the centroids of the chromone rings vary between approximately 3300 and 4100 Å. This indicates that the rings are not perfectly aligned and have considerable displacement, which is typical of π - π offset/slipped interactions. The shortest distances are present in compounds such as 3 and 5, while the longest distances are observed in compounds 9 and 10. This suggests that compounds with longer distances could have interactions π - π weaker. Likewise, the vertical displacements are close to the distances between the centroids, which indicates that the interaction π - π is not perfectly stacked, but rather displaced (slipped). The values of vertical distance from the ring centroid (R1V and R2V) indicate a parallel displacement pattern, typical of π - π interactions in many aromatic compounds. In some compounds such as 10 and 26, the vertical distance values show little variation (e.g., 3.445 and 3.474 Å), which could imply relatively good alignment, but with possible weaker interactions than in compounds

with smaller distances. Moreover, compounds with larger angles and distances, such as compound 9, show weaker π - π interactions, which could affect the stability of structures in biological systems or materials. Likewise, small angles as in compound 3 ($\alpha = 1^\circ$, $\beta = 4.5^\circ$, $\gamma = 5.7^\circ$) suggest a near-perfect overlap of the rings, which favors an interaction π - π stabilizing.

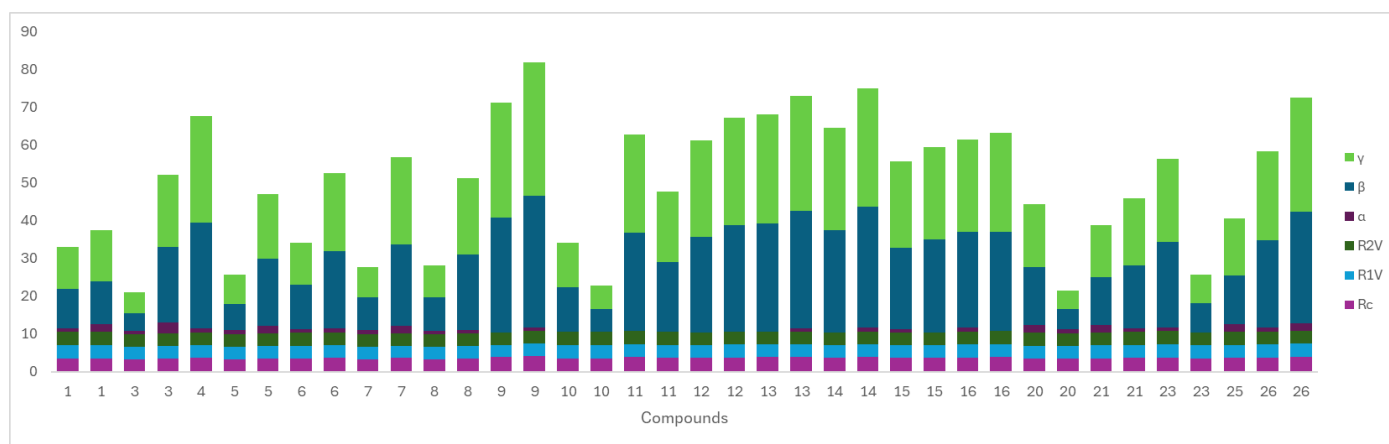


Figure 2. Geometric parameters that involving π - π interactions (A° , $^\circ$) between heterocycles of chromone ring of 1, 3–16, 20–23, 25 and 26 compounds.

To synthesize the information presented, compound 8, whose molecular structure is shown in Figure 1, is taken as a representative example. The complete crystallographic information can be found in CCDC under number 1007014.

In the crystal, the molecules that are united through hydrogen bonds $C-H \cdots O$ y $C-H \cdots F$, they form supramolecular arrays from of rings arrays $R_2^2(8)$ and $R_2^3(10)$, in this last one we can observe that an equal hydrogen atom connects through hydrogen bonds an oxygen atom and a fluorine atom, forming a 10-membered ring, see Figure 3. The energies that contribute most to the spontaneous nature of these interactions are dispersive and electrostatic with values between -11 and -15.9 kJ/mol.

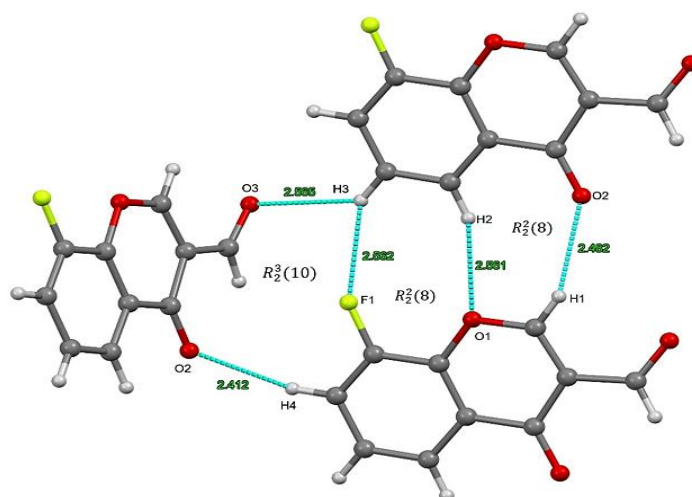


Figure 3. Hydrogen bonding interaction $C-H \cdots O$ and $C-H \cdots F$ (light blue dashed line) of the 8 compound.

It can also be observed $\pi \cdots \pi$ (stacking) interactions between the pyran and phenyl ring planes such that an offset/slipped conformation is generated where the angles meet the following $0^\circ = \alpha < \beta = \gamma$; $C_g - C_g = C_g I_{perp} = C_g J_{perp}$. The molecule also exhibits

C—O \cdots π interactions depicted in Figure 4 that trace molecular planes perpendicular to each other. Both interactions act cooperatively to stabilize the crystal lattice.

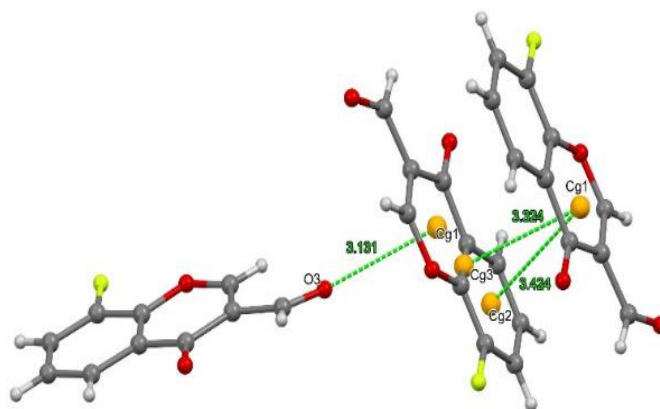


Figure 4. π \cdots π stacking and C—O \cdots π interactions (green dashed plot) showing intercentroid interaction and O \cdots Cg1 distance of the 8 compound.

3.2. Hirshfeld Surface Analyses

The main intermolecular interactions of the crystal were quantified using Hirshfeld surface analyses. Figure 5 shows the d_{norm} surface, it presents a frontal view and a 180° rotation around the x-axis (horizontal of surfaces) where the red colored regions evidence close hydrogen bridge type contacts C—H \cdots O and C—H \cdots F indicated by arrows numbered 1 and 2 respectively.

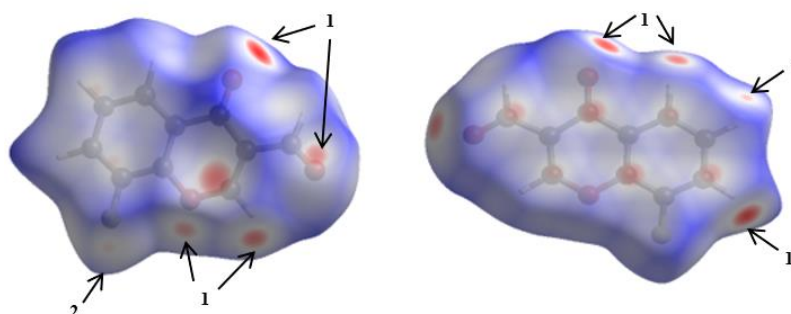


Figure 5. View of Hirshfeld surfaces in two orientations for compound 8. (1) C—H \cdots O; (2) C—H \cdots F of the 8 compound.

The shape index and curvedness properties are illustrated in Figure 6. These properties help to identify and visualize planar stacking arrangements. The alternating red and blue bowtie-shaped triangles observed on the surfaces generated with the shape index property are evidence of π \cdots π stacking arrangements in the crystal lattice. The red colored triangles are concave regions associating ring atoms located above, giving rise to π \cdots π stacking interactions, while the blue colored triangles are convex regions indicating aromatic ring atoms of the molecule within the surface. Similarly, the π \cdots π interactions are evident as relatively broad flat regions of green color, bounded by blue contours of the surfaces resulting from the curvature index or curvedness.

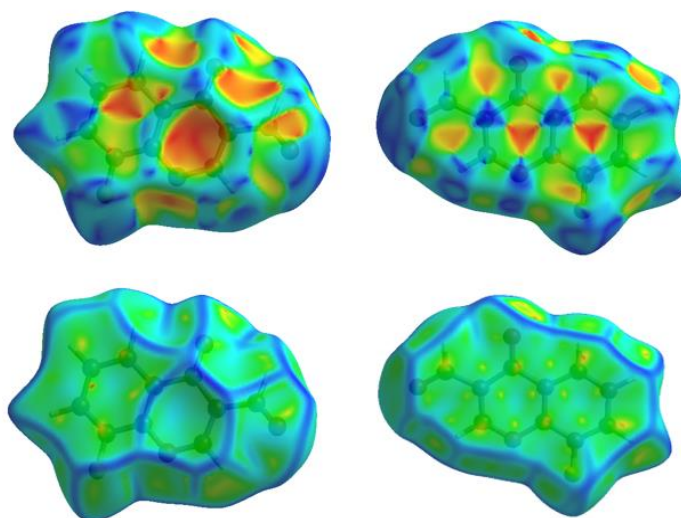


Figure 6. Hirshfeld surfaces evaluated with the shape index and curvature (curvedness) of the **8** compound.

Figure 7 shows the 2D decomposition graph (fingerprint). The intermolecular contacts are marked with numbers on the surface. The pair of sharp peaks with number 1 corresponds to the shorter O \cdots H interactions associated with C–H \cdots O hydrogen bonds, number 2 shows the presence of F–H contacts of the C–H \cdots F type. The green colored region with number 4 in the center of the surface indicates the presence of C \cdots C contact, evidencing the π \cdots π stacking between the phenyl rings of the chromone core, these results correlate with those observed in the shape index and curvature (curvedness) described above.

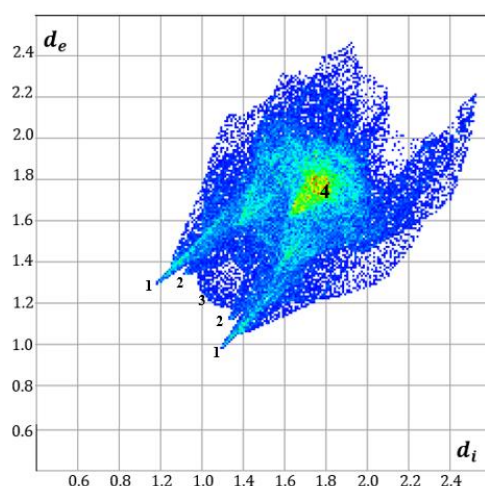


Figure 7. 2D fingerprint plot of the close contacts with the greatest contribution as (1) O \cdots H, (2) F \cdots H (3) H \cdots H and (4) C \cdots C of the **8** compound.

The relative contributions of the intermolecular contacts on the Hirshfeld surface for the set of compounds to which compound **8** belongs are shown in Figure 8. It is observed that they share a main contribution (15–40%) corresponding to the F \cdots H interaction [11], due to the high proportion of terminal fluorine atoms in all the molecules, which suggests a clear preference of interaction between hydrogen atoms with fluorine atoms [12–15]. The second relative contribution (12–32%) is that generated by O \cdots H contact, which associates the classical hydrogen bond C–O \cdots H. It is inferred that the presence of the carbonyl group in compound **8** favors this type of intermolecular contacts due to the nature of the

aldehyde group. The other contacts of minor contribution also help to stabilize the crystal lattice and correspond to weak C ... F, O ... O, O ... F, F ... F contacts.

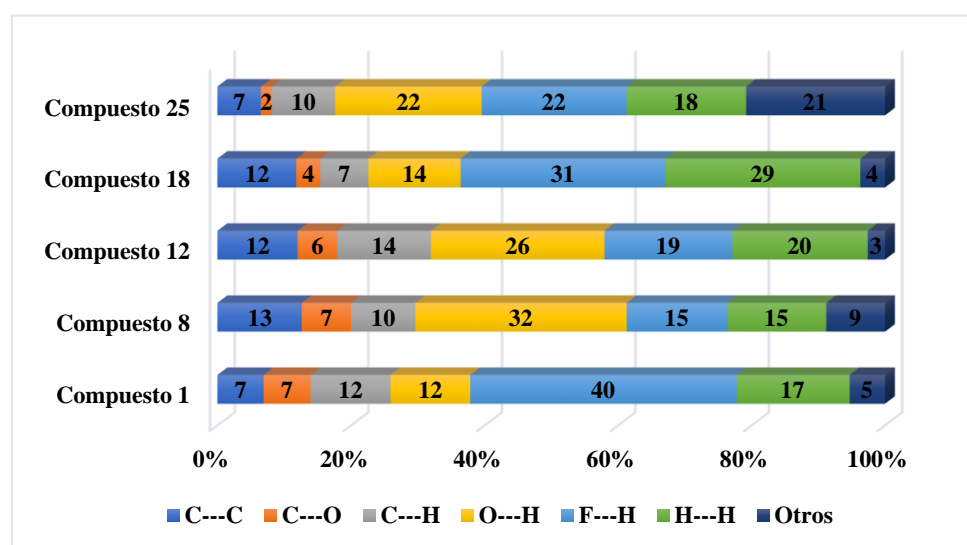


Figure 8. Relative contributions of the main intermolecular contacts on the Hirshfeld surface for the set of compounds.

4. Conclusions

The studied molecules present halogen type bonds that border a distance of 3.00–4.00 Å. Also, $\pi \cdots \pi$ stacking interactions between the centroids of the rings and C–X $\cdots \pi$ interactions that participate in the stabilization of the crystal and preference in the crystalline packing are observed. In the hydrogen and halogen bonds it was observed that the electrostatic and dispersive energies have higher values compared to the polarization energies and the total energy, which suggests that the formation of this type of bonds is mainly due to the first two energies mentioned above.

Specifically compound 8 presented non-classical hydrogen bond intermolecular interactions forming supramolecular arrangements of $R_2^2(8)$ and $R_3^3(10)$ ring sets. $\pi \cdots \pi$ stacking and C–O $\cdots \pi$ interactions were also present in the molecular structure. Hirshfeld surface analyses corroborated the presence of all these interactions, d_{norm} surface indicates the C–O \cdots H bonds occurring in pyran ring and aldehyde group, contributing 32% to the surface. The C–H \cdots F and C–H \cdots H bonds contributed 15%. The surface shape index showed the presence of stacking $\pi \cdots \pi$ bonds in the form of alternating red and blue triangles in the pyran and phenyl rings.

The presence of these interactions gives reason for the potential biological activity and its incidence in the processes of self-assembly in small molecules as well as in large biological systems, which generates stability in the crystalline structure, allowing them to be the object of study for the elaboration of drugs and new materials.

Author Contributions: Conceptualization, L.A.H.-S., C.D.A.-L. and P.M.B.-V.; investigation, L.A.H.-S. and C.D.A.-L.; writing—original draft preparation, L.A.H.-S. and C.D.A.-L.; writing—review and editing, L.A.H.-S. and C.D.A.-L.; supervision, C.D.A.-L. and P.M.B.-V.; project administration, C.D.A.-L. All authors have read and agreed to the published version of the manuscript.

Funding: This research received no external funding.

Institutional Review Board Statement: Not applicable.

Informed Consent Statement: Not applicable.

Data Availability Statement: All data generated or analyzed during this study are included in this published article.

Conflicts of Interest: The authors declare no conflicts of interest.

References

1. Gaspar, A.; Garrido, E.M.P.J.; Borges, F.; Garrido, J.M.P.J. Biological and Medicinal Properties of Natural Chromones and Chromanones. *ACS Omega* **2024**, *9*, 21706–21726. <https://doi.org/10.1021/acsomega.4c00771>.
2. Mohsin, N.U.A.; Irfan, M.; Hassan, S.U.; Saleem, U. Current Strategies in Development of New Chromone Derivatives with Diversified Pharmacological Activities: A Review. *Pharm. Chem. J.* **2020**, *54*, 241–257. <https://doi.org/10.1007/s11094-020-02187-x>.
3. Sosnovskikh, V.Y. Synthesis and Reactions of Halogen-Containing Chromones. *Russ. Chem. Rev.* **2003**, *72*, 489–516. <https://doi.org/10.1070/RC2003v072n06ABEH000770>.
4. Sosnovskikh, V.Y.; Usachev, B.I. 2-Polyfluoroalkylchromones. 5. Nitration and Chlorination of 2-Trifluoromethylchromones. *Russ. Chem. Bull.* **2000**, *49*, 2074–2076. <https://doi.org/10.1023/A:1009544630187>.
5. Sosnovskikh, V.Y.; Korotaev, V.Y.; Chizhov, D.L.; Kutyashev, I.B.; Yachevskii, D.S.; Kazheva, O.N.; Dyachenko, O.A.; Charushin, V.N. Reaction of Polyhaloalkyl-Substituted Chromones, Pyrones, and Furanones with Salicylaldehydes as a Direct Route to Fused 2H-Chromenes. *J. Org. Chem.* **2006**, *71*, 4538–4543. <https://doi.org/10.1021/jo060459x>.
6. Duan, Y.; Jiang, Y.; Guo, F.; Chen, L.; Xu, L.; Zhang, W.; Liu, B. The Antitumor Activity of Naturally Occurring Chromones: A Review. *Fitoterapia* **2019**, *135*, 114–129. <https://doi.org/10.1016/j.fitote.2019.04.012>.
7. Pastuszko, A.; Majchrzak, K.; Czyz, M.; Kupcewicz, B.; Budzisz, E. The Synthesis, Lipophilicity and Cytotoxic Effects of New Ruthenium(II) Arene Complexes with Chromone Derivatives. *J. Inorg. Biochem.* **2016**, *159*, 133–141. <https://doi.org/10.1016/j.jinorgbio.2016.02.020>.
8. Zhu, Y.; Yao, X.; Long, J.; Li, R.; Liu, Y.; Yang, Z.; Zheng, X. Fluorine-Containing Chrysin Derivatives: Synthesis and Biological Activity. *Nat. Prod. Commun.* **2019**, *14*, 1934578X19878921. <https://doi.org/10.1177/1934578X19878921>.
9. Priimagi, A.; Cavallo, G.; Metrangolo, P.; Resnati, G. The Halogen Bond in the Design of Functional Supramolecular Materials: Recent Advances. *Acc. Chem. Res.* **2013**, *46*, 2686–2695. <https://doi.org/10.1021/ar400103r>.
10. Jaime-Adán, E.; Hernández-Ortega, S.; Toscano, R.A.; Germán-Acacio, J.M.; Sánchez-Pacheco, A.D.; Hernández-Vergara, M.; Barquera, J.E.; Valdés-Martínez, J. Competition of Hydrogen Bonds, Halogen Bonds, and π - π Interactions in Crystal Structures. Exploring the Effect of One Atom Substitution. *Cryst. Growth Des.* **2024**, *24*, 1888–1897. <https://doi.org/10.1021/acs.cgd.3c00910>.
11. Narváez, O.E.G.; Bonilla, V.P.M.; Zurita, D.A.; Alcívar, L.C.D.; Heredia-Moya, J.; Ulic, S.E.; Jios, J.L.; Piro, O.E.; Echeverría, G.A.; Langer, P. Synthesis, Experimental and Theoretical Study of Novel 2-Haloalkyl (-CF₂H, -CCl₂H, -CF₂CF₃)-, 3-Bromo and Bromomethyl Substituted Chromones. *J. Fluor. Chem.* **2021**, *242*, 109717. <https://doi.org/10.1016/j.jfluchem.2020.109717>.
12. Alcívar León, C.D.; Piro, O.E.; Echeverría, G.A.; Ulic, S.E.; Jios, J.L. Synthesis and Conformational Theoretical Study of Novel Derivatives of 2-(Trifluoromethyl)Chromone: 3-Cyanomethyl and 3-Aminomethyl 2-(Trifluoromethyl)Chromones. *J. Argent. Chem. Soc.* **2014**, *101*.
13. Alcívar León, C.D.; Echeverría, G.A.; Piro, O.E.; Ulic, S.E.; Jios, J.L. A Detailed Experimental and Theoretical Study of Two Novel Substituted Trifluoromethylchromones. The Influence of the Bulky Bromine Atom on the Crystal Packing. *Spectrochim. Acta A Mol. Biomol. Spectrosc.* **2015**, *136*, 1358–1370. <https://doi.org/10.1016/j.saa.2014.10.022>.
14. Alcívar León, C.D.; Echeverría, G.A.; Piro, O.E.; Ulic, S.E.; Jios, J.L.; Burgos Paci, M.; Argüello, G.A. The Role of Halogen C-X₁...X₂-C Contact on the Preferred Conformation of 2-Perhalomethylchromones in Solid State. *Chem. Phys.* **2016**, *472*, 142–155. <https://doi.org/10.1016/j.chemphys.2016.03.017>.
15. Alcívar León, C.D.; Echeverría, G.A.; Piro, O.E.; Ulic, S.E.; Jios, J.L.; Pereañez, J.A.; Henao Castañeda, I.C.; Pérez, H. The Role of Non-Covalent Interactions in Some 2-Trifluoromethylchromones in the Solid State. *New J. Chem.* **2017**, *41*, 14659–14674. <https://doi.org/10.1039/c7nj00481h>.

Disclaimer/Publisher's Note: The statements, opinions and data contained in all publications are solely those of the individual author(s) and contributor(s) and not of MDPI and/or the editor(s). MDPI and/or the editor(s) disclaim responsibility for any injury to people or property resulting from any ideas, methods, instructions or products referred to in the content.